J. Chem. Sci. Vol. 123, No. 5, September 2011, pp. 743–754.

A density functional study on the adsorption of hydrogen molecule onto small copper clusters

XIANG-JUN KUANG[a,b,*], XIN-QIANG WANG[a,*] and GAO-BIN LIU[a]

[a]College of Physics, Chongqing University, Chongqing, 400044, China

[b]School of Science, Southwest University of Science and Technology, Mianyang, Sichuan 621010, China

e-mail: kuangxiangjun@163.com; xqwang@cqu.edu.cn

MS received 25 July 2010; revised 20 May 2011; accepted 27 May 2011

Abstract. An all-electron scalar relativistic calculation on the adsorption of hydrogen molecule onto small copper clusters has been performed by using density functional theory with the generalized gradient approximation (GGA) at PW91 level. Our results reveal that after adsorption of H_2 molecule, the Cu–Cu interaction is strengthened and the H–H interaction is weakened, the reactivity enhancement of H_2 molecule is obvious. The VIPs, HLGs and VEAs of Cu_nH_2 clusters show an obvious odd–even oscillation. It is suggested that the H_2 molecule is more favourable to be adsorbed by the even-numbered small copper clusters. Meanwhile, the odd–even alteration of magnetic moments is also observed and may be served as the material with tunable code capacity of '0' and '1' by adsorbing hydrogen molecule onto odd or even-numbered small copper clusters. Some discrepancies of dissociative adsorption between our work and previous works are found and may be understood in terms of the electron pairing effect and the scalar relativistic effect.

Keywords. Small copper cluster; hydrogen molecule; adsorption; all-electron scalar relativistic calculation.

1. Introduction

Theoretical investigations of catalyses are difficult primarily because the involved reactions only occur at infinite surface. This makes it necessary to compromise between the solid state and cluster physics. Starting from the initial works of Upton *et al.*[1,2] and Bauschlicher *et al.*,[3] one common solution is to use small metal clusters as models for the infinite metal surface. This has attracted a great deal of attention and has been widely used in numerous theoretical investigations of atomic and molecular adsorption onto metallic systems. Gold, one kind of coinage metal element and known as an inert material in bulk form, is found to be active with a cluster size below 3–4 *nm*. The adsorption behaviour of small molecules, such as O_2, N_2, H_2, CO and NO onto small gold clusters, has been studied experimentally and theoretically.[4–8] It is found that the adsorption behaviour of these molecules onto gold clusters strongly depends on the charge states and the size of gold clusters.

The increased catalytic activities of clusters with confined sizes seem to be not limited to Au, but also relevant for other coinage metal clusters. For example, Ag and Cu clusters are found to show similar catalytic activities with those of Au clusters for the partial oxidation of hydrocarbons and low temperature CO-oxidation, implying that the high catalytic activities of small clusters also can be relevant for other coinage metal clusters such as Ag and Cu.[9,10] Therefore, studies on the adsorption behaviour of Ag and Cu clusters can also provide important information to better understand catalytic process of Ag and Cu-based nanocatalysis. In fact, there are some studies on the adsorption behaviour of H, H_2, O_2 and CO onto small Cu clusters experimentally and theoretically.[11–16] Guvelioglu *et al.* have systematically studied the structural evolution of small copper clusters up to 15 atoms and the dissociative adsorption of H_2 onto the minimum energy copper clusters by using the density functional theory.[11] They identify that Cu_4 gives the highest adsorption energy for dissociative adsorption of H_2 and the adsorption energy decreases as the clusters evolve. To understand the evolution of small copper clusters, they have also performed a calculation on selected icosahedral clusters (for $n = 13, 19, 25, 55$) and fcc-like clusters ($n = 14, 23, 32, 41$).[12] By extrapolating and interpolating the binding energies of triangular clusters, icosahedral clusters and bulk-like clusters, they find that structural transitions from the triangular growth clusters to

*For correspondence

the icosahedral and fcc-like clusters occur at approximately $n = 16$ and $n = 32$, respectively. Subsequently, they perform an extensive calculation on the dissociative adsorption of H_2 on the minimum energy clusters. The adsorption likely occurs near the most acute metal site with the two H atoms residing on the edges, which differs significantly from the adsorption on Cu surfaces that usually takes place at the hollow sites. By using both all-electron and one-electron effective core potential methods, Triguero *et al.*[13] have studied the hydrogen atom adsorption on geometry optimized copper clusters with up to nine copper atoms and find that the adsorption energy on the odd-numbered clusters are of the order of 20 kcal/mol higher than that on the even-numbered clusters. Campos[14] has performed a theoretical study of molecular oxygen and atomic oxygen adsorption onto small Cu clusters by using density functional theory. His results indicate that the molecular oxygen reactivity is dependent on the odd–even alternation of the number of copper atoms in the cluster, Cu clusters with odd number of atoms exhibit the highest reactivity in general. A similar behaviour is found for the atomic oxygen adsorption onto the same copper clusters. And then, Campos also carries out a theoretical study on the adsorption of carbon monoxide onto small Cu_n ($n = 1$–8) clusters.[15] When the CO molecule approaches perpendicularly to the adsorption site, it is adsorbed on a top site (one-fold coordination), presenting a high degree of symmetry in the adsorption system. The reactivity of the CO molecule is independent of the even–odd alternation with respect to the number of atoms of copper in the cluster. Holmgren *et al.*[16] have investigated the reactivity of Cu clusters with NO by using the laser-vaporization source, low-pressure reaction cell and photoionization time-of-flight mass spectrometer. The reactivity of Cu clusters toward NO is very low overall for $n = 15$–41, whereas the reactivity is higher for the larger clusters and is strongly size selective in the range of $n = 40$–60, with particularly high relative reactivity of Cu_{53} and Cu_{54}.

Although there are some studies on the dissociative adsorption behaviour of hydrogen molecule onto small copper clusters[11,12] and the hydrogen atom adsorption onto small copper clusters,[13] few are available to show the influence of scalar relativistic effect on the adsorption behaviour of small copper clusters. Previous studies[17–21] indicate that for coinage metal element, the scalar relativistic effect of outer shell electrons is obvious and may cause the shrink of the size of s orbitals and the expansion of size of d, f orbitals, and thus enhance the s–d hybridization. The reason for the preference of planar structures by some coinage metal clusters up to large size may be attributed to the scalar relativistic effect of outer shell electrons. The scalar relativistic effect has the obvious influence on the properties of coinage metal clusters and should be included in the studying of the adsorption behaviour for these clusters. In this paper, we choose an interesting and well-defined system as a case to perform an all-electron scalar relativistic (AER) calculation on the hydrogen molecule adsorption onto Cu_n ($n = 1$–13) clusters by using density functional theory with the generalized gradient approximation (GGA) at PW91 level. Hydrogen is the first element in periodic table with the atomic configuration of $1s^1$ and copper has the atomic configuration of $3d^{10}\ 4s^1$. It is very interesting to study the interaction between small copper cluster and hydrogen molecule because both Cu and H only have single s valence electron. The objectives of present study are the following: (i) to investigate the hydrogen molecule adsorption effect on the geometrical structures, the electronic and magnetic properties of small copper clusters, (ii) examine the influence of scalar relativistic effect on the adsorption behaviour of small copper clusters by comparing with the previous works. The paper is arranged as follows: the computational method and cluster model are described in section 2, calculation results and discussions are presented in section 3, and the main conclusions are summarized in section 4.

2. Computational method and cluster model

The geometrical structures, electronic and magnetic properties of Cu_nH_2 ($n = 1$–13) clusters are calculated by using the density functional theory (DFT). Under the framework of DFT, the scalar relativistic effect will be included because of the reason described in section 1. The numerical atomic orbitals are used in construction of molecular orbitals. In many previous cases, as an approximation, only the outer shell atom-orbitals are employed to generate the valence orbitals and the rest of the core orbitals are frozen. Although the calculations involving all-electron scalar relativistic (AER) method are more difficult to perform due to the huge computational expense, they are supposed to provide better accuracy than those involving effective core potentials. The advantages of the all-electron scalar relativistic (AER) method over the effective core potential method have been demonstrated by some early works.[22–24] Considering above factors and in order to improve the calculation accuracy, we have carried out an all-electron

Table 1. Comparison of results among all-electron scalar relativistic (AER) calculation, all-electron (AE) calculation and effective core potential (ECP) calculation for Cu_3H, Cu_3 and Cu_4 clusters.

Cluster	Cu_3H				Cu_3	Cu_4
	E_b(eV/atom)	r_{Cu-Cu}(Å)	r_{Cu-H}(Å)	ν_{Cu-H}(cm^{-1})	E_b (eV/atom)	E_b (eV/atom)
Exp	1.610	2.330	1.480	1913.5	1.190	1.620
AER	1.604	2.359	1.502	1891.4	1.187	1.580
AE	1.524	2.388	1.522	1808.5	1.103	1.493
ECP	1.540	2.409	1.511	1820.1	1.111	1.440

scalar relativistic (AER) calculation and used the corresponding high quality DNP basis set despite of the huge computational expense.

The PW91 form of GGA for the exchange-correlation functional is adopted in the calculation, and the SCF tolerance is set to be 1.0×10^{-6} eV. In order to accelerate the calculation, the direct inversion in iterative subspace (DIIS) approach is used and the smearing value is set to be 0.005 *Ha*. During the structure optimization, the spin is unrestricted and the symmetry of the structure has no constraint. The convergence tolerance of max force, max energy and max displacement is 0.002Ha/Å, 1.0×10^{-5}Ha and 0.005 Å, respectively. During the structure relaxation, the spin multiplicity will be considered at least 1, 3 and 5 for even-electron Cu_nH_2 clusters (n = 2, 4, 6, 8, 10 and 12) and 2, 4, 6 for odd-electron Cu_nH_2 clusters (n = 1, 3, 5, 7, 9, 11 and 13). If the total energy decrease with the increasing of spin multiplicity, the high spin state will be considered until the energy minimum with respect to the spin multiplicity is reached. In addition, the stability of the optimized geometry is confirmed without any imaginary frequency by computing vibrational frequencies at the same level of theory.

The choice of distinct initial geometries is important to the reliability of obtained lowest energy structures. In this work, we get the initial structures by the following way: First, considering previous studies on the configurations of pure copper clusters,[25–30] we optimize the structures of pure Cu_n clusters by using the same method and same parameters. Then, on the basis of the optimized equilibrium geometries of pure copper clusters, we obtain the initial structures of Cu_nH_2 clusters by making H_2 molecule approach to each non-equivalent adsorption site of Cu_n cluster molecularly, including all possible bonding patterns. All these initial structures are fully optimized by relaxing the atomic positions until the force acting on each atom vanishes (typically $F_i \leq$ 0.002Ha/ Å) and by minimizing the total energy.

In order to check the intrinsic reliability of the computational method, we chose Cu_3, Cu_4 and Cu_3H (the corresponding experimental data available) as examples to calculate some properties of these clusters by using all-electron scalar relativistic (AER) method, all-electron (AE) method and effective core potential (ECP) method, respectively. From the calculation results listed in table 1, we can find that the results obtained by AER are more close to the available experimental data[31–33] than those of obtained by AE and ECP method. This indicates that AER method is more reliable and more accurate for the studying of Cu_nH_2 clusters than the AE and ECP method.

3. Results and discussion

3.1 *Geometrical and electronic structures*

In order to acquire the initial structures of Cu_nH_2 clusters, we optimize the pure Cu_n clusters first, the lowest energy geometries of pure Cu_n (n = 2–13) cluster shown in figure 1 are in good agreement with available previous works.[25–30] Then, based on the optimized lowest energy structures of Cu_n clusters, we perform an extensive lowest energy structures search for hydrogen molecule bonding onto Cu_n cluster according to the way described in section 2. The lowest energy geometries for Cu_nH_2 (n = 1–13) clusters are displayed in figure 2. When H_2 molecule approaches to single Cu atom and is molecularly adsorbed to be CuH_2 cluster with linear structure, only one H atom prefers to bond with Cu atom. When H_2 molecule approaches to Cu_n (n = 2–9) clusters and is molecularly adsorbed to be Cu_nH_2 (n = 2–9) clusters. The two H atoms prefer to bond with same one Cu atom. When H_2 molecule approaches to other Cu_n (n = 10–13) clusters, the H–H distance is elongated so large that the H_2 molecule is dissociated with two H atoms residing on

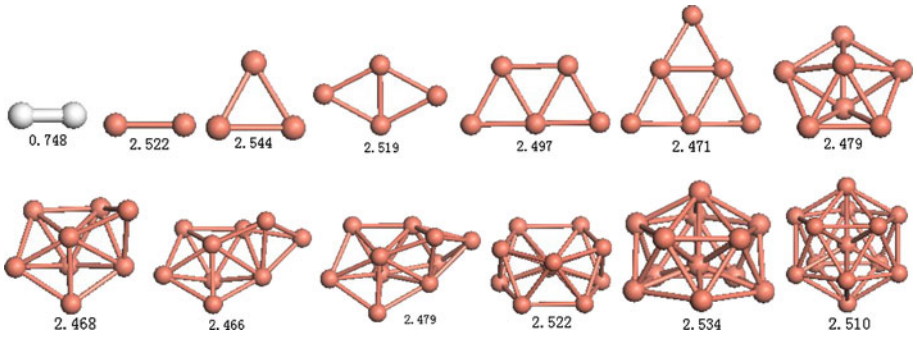

Figure 1. Lowest energy geometries for single H_2 molecule and pure Cu_n (n = 2–13) clusters. The average Cu–Cu bond-length of pure Cu_n (n = 2–13) cluster and the H–H bond-length of single H_2 molecule in angstrom are shown next to each cluster.

the two sides of sharp corner Cu atom. The two dissociated H atoms prefer to occupy the two or three-fold coordination site and are found to be favourable to bonding with four and five-coordinated Cu atoms. No dissociative adsorption takes place on six-coordinated or other high coordinated Cu atoms. The low-coordinated Cu atoms seem to be more reactive toward H_2 molecule. This situation is consistent with the dissociative adsorption of H_2 onto small gold clusters[34] and may be understood in terms of the lack of charge transfer channels and electron pairing chance. In all these cases, the H–H bond of the adsorbed H_2 is elongated. It is consistent with the Kubas-type interaction scheme and suggests some contribution from Kubas bonding of hydrogen molecules to the adsorption sites.[35,36] Compared with pure Cu_n clusters, the Cu_{11} structure in $Cu_{11}H_2$ cluster is distorted obviously. But, in other Cu_nH_2 clusters, the Cu_n structures are perturbed and distorted slightly. This picture is very different from previous work[11] in which the adsorption gives rise to considerable structural change for all small clusters and only moderate perturbation for larger ones. Besides the obvious lengthening of H–H distances, the Cu–Cu bond-length in Cu_nH_2 cluster is

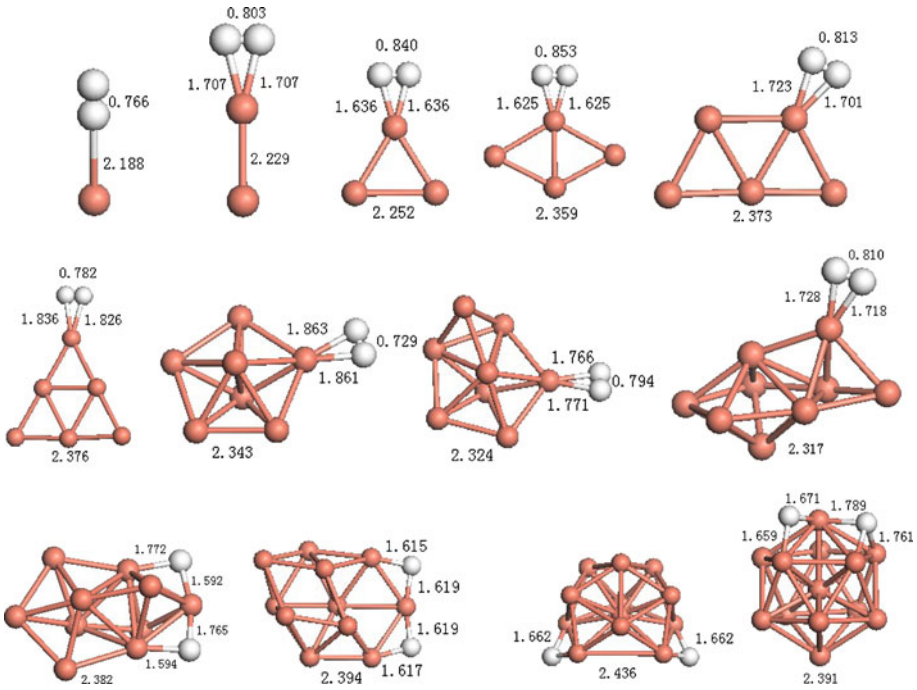

Figure 2. Lowest energy geometries for Cu_nH_2 (n = 1–13) clusters. The average Cu–Cu bond-length and Cu–H bond-length in angstrom are shown next to each cluster.

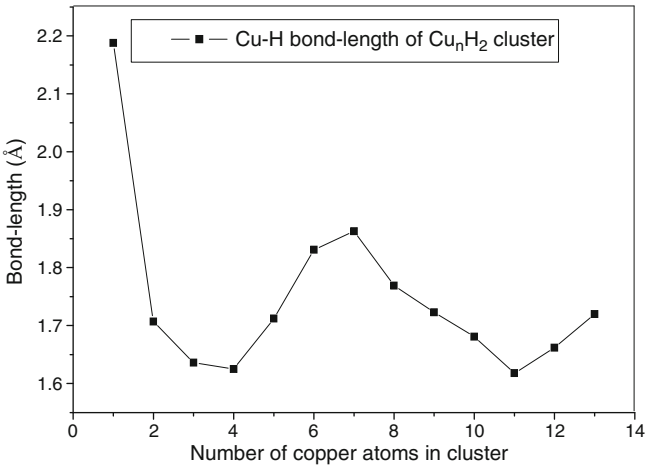

Figure 3. Size dependence of Cu–H bond-length for Cu_nH_2 cluster.

shorter than that in corresponding pure Cu_n cluster. It is inferred that the Cu–Cu interaction is strengthened and the H–H interaction is significantly weakened after adsorption. This situation can be explained in terms of the electron donation and electron back donation between the hybridized orbital of Cu_n and the hybridized orbital of H_2 molecule, which results the better overlap between these orbitals and the enhancement of interaction between small copper cluster and H_2 molecule. Meanwhile, with the increasing number of copper atoms, the Cu–H bond-length fluctuates in a wave-like manner and reaches the minimum value of 1.618 Å at $n = 11$ and maximum value of 2.188 Å at $n = 1$(see figure 3). This indicates that the strongest adsorption might exist in $Cu_{11}H_2$ cluster and the weakest adsorption might exist in CuH_2 cluster. Triguero *et al*. have studied the Cu_nH ($n = 2$–9) clusters by using both all-electron and one-electron effective core potential methods.[13] From table 2 and figure 2, we can easily find that the Cu–Cu bond-length of the lowest energy geometry of Cu_nH_2 ($n = 1$–13) cluster in our work is significantly shorter than that of Cu_nH ($n = 2$–9) cluster in previous work.[13] This discrepancy tells us that hydrogen molecule adsorption is more favourable to enhancement of Cu–Cu interaction than the hydrogen atom adsorption. It can be explained in terms of the electron pairing effect. Compared with the single hydrogen atom adsorption, the charge transfer between hydrogen molecule and copper cluster is greater. This situation can give more electron pairing chance for the unpaired valence electrons in copper cluster and is favourable to the adsorption. Meanwhile, compared with the previous work of ref.[11], the dissociative adsorption only takes place in some Cu_nH_2 ($n = 10$–13) clusters of our work and not in all Cu_nH_2 ($n = 2$–15) clusters like ref.[11]. Different from ref.[11], the Cu_{11} gives the largest adsorption energy for dissociative adsorption of H_2 and the Cu_4 gives the largest adsorption energy for molecular adsorption of H_2 in our work. These discrepancies may be explained in terms of the scalar relativistic effect. The scalar relativistic effect leads to the shrink of the size of *s* orbitals and the expansion of the size of *d*, *f* orbitals.[17–21] The *sd* hybridization in Cu_n cluster or between the *s*, *d* orbital of Cu_n cluster and the *s* orbital of H_2 molecule becomes stronger. With the increasing size of copper cluster, the influence of scalar relativistic effect on the adsorption behaviour is becoming stronger. The strengthening of Cu–Cu interaction and the weakening of H–H interaction are more obvious, the reactivity of Cu_n

Table 2. Some calculated energy data of our work and the Cu–Cu bond-length from Ref.[13]

Cluster	BE (eV/atom)		E_{ads}(eV)	HLG (eV)	VIP (eV)	VEA (eV)	η (eV)	r_{Cu-Cu} (Å) Ref[13]
	Cu_n	Cu_nH_2						
CuH_2	0.000	1.594	0.113	0.718	7.846	0.684	3.581	
Cu_2H_2	1.055	1.726	0.451	2.625	7.904	0.169	3.868	2.591
Cu_3H_2	1.187	1.829	0.583	0.638	6.163	0.549	2.807	2.473
Cu_4H_2	1.580	1.909	0.705	2.002	6.882	0.222	3.330	2.620
Cu_5H_2	1.724	1.973	0.328	0.442	6.273	1.264	2.504	2.534
Cu_6H_2	1.909	2.038	0.184	1.899	6.585	0.767	2.909	2.759
Cu_7H_2	2.032	2.117	0.135	0.368	5.992	1.303	2.345	2.555
Cu_8H_2	2.105	2.176	0.250	1.223	6.133	1.296	2.419	2.555
Cu_9H_2	2.118	2.235	0.304	0.214	5.957	1.752	2.102	2.555
$Cu_{10}H_2$	2.202	2.293	0.822	1.419	6.329	1.395	2.467	
$Cu_{11}H_2$	2.260	2.308	1.577	0.283	5.912	1.822	2.045	
$Cu_{12}H_2$	2.315	2.324	1.281	0.583	6.305	1.452	2.427	
$Cu_{13}H_2$	2.353	2.375	1.236	0.103	5.887	2.021	1.933	

cluster toward H_2 molecule is enhanced gradually, appearing as the shortening of Cu–Cu bond-length and the lengthening of H–H bond-length.

3.2 *Energy and electronic structure*

Some calculated energy data for Cu_nH_2 clusters are listed in table 2, where the binding energy (BE) per atom, adsorption energy E_{ads}, vertical ionization potential (VIP) and vertical electron affinity (VEA) are defined as follows:

$$BE(Cu_nH_2) = [nE(Cu) + 2E(H) - E(Cu_nH_2)]/(n+2)$$
$$E_{ad} = [E(Cu_n) + E(H_2) - E(Cu_nH_2)]$$
$$VIP = E(Cu_nH_2)^+ - E(Cu_nH2)$$
$$VEA = E(Cu_nH_2) - E(Cu_nH2)^-.$$

Generally speaking, the binding energy of a given cluster is a measurement of its thermodynamic stability. From table 2 and figure 4, we can find that the binding energy of Cu_nH_2 cluster is larger than that of corresponding pure copper cluster. With increasing number of copper atoms, the binding energy of pure copper cluster increases gradually and reaches the maximum value of 2.353 eV at $n = 13$. Meanwhile, the binding energy of Cu_nH_2 cluster also increases gradually and reaches the maximum value of 2.375 eV at $n = 13$ too. However, the binding energy difference between Cu_nH_2 and Cu_n cluster becomes small gradually. This indicates that the adsorption of hydrogen molecule enhances the stability of pure copper cluster energetically. With increasing number of copper atoms, the stability of Cu_nH_2 cluster is increased gradually like the increasing stability of pure copper cluster. But, the stability enhancement effect of hydrogen molecule adsorption becomes weakened gradually with increasing size of Cu_nH_2 cluster.

From the adsorption energy between Cu_n and H_2 listed in table 2 and displayed in figure 4, we can see that with increasing number of copper atoms, the adsorption energies fluctuate in a wave-like manner with the opposite variation tendency of Cu–H bond-lengths and reach the maximum value of 1.577 eV at $n = 11$ and the minimum value of 0.113 eV at $n = 1$ (see table 2 and figure 4). This situation is consistent with the shortest Cu–H bond-length in $Cu_{11}H_2$ cluster and longest Cu–H bond-length in CuH_2 cluster. It is proved again that the strongest adsorption exists in $Cu_{11}H_2$ cluster and the weakest adsorption exists in CuH_2 cluster.

Vertical ionization potential (VIP) is often used to investigate the chemical stability of small clusters, the larger of the VIP, the deeper (higher) of the HOMO (LUMO) energy level, which leads to less reactivity or higher chemical stability. HOMO–LUMO gap (HLG) is another useful parameter for examining the electronic stability of a cluster. The larger of HLG, the higher energy is required to excite the electrons from valence band to conduction band, corresponding to higher stability of electronic structure. Vertical electron affinity (VEA) is also a means for the evaluation of the relative stability of cluster with different size. A higher vertical electron affinity means that more energy is released when an electron is added to a neutral molecule and the production of the corresponding anion is more readily accomplished. A neutral cluster with smaller vertical electron affinity is generally more stable. From the data listed in table 2 and shown in figure 5, we can

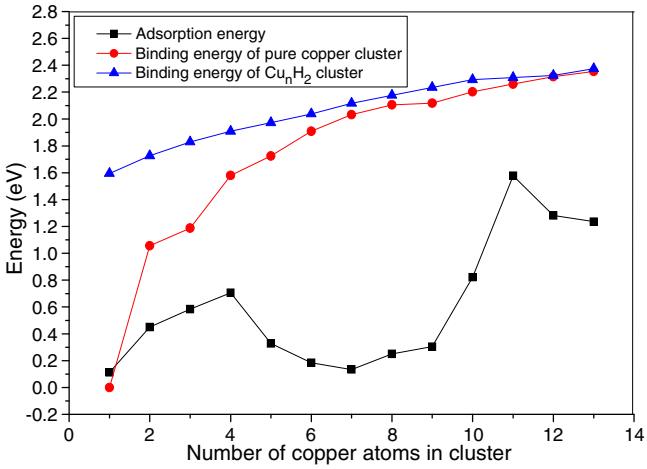

Figure 4. Size dependence of binding energy and adsorption energy for Cu_nH_2 and pure Cu_n cluster.

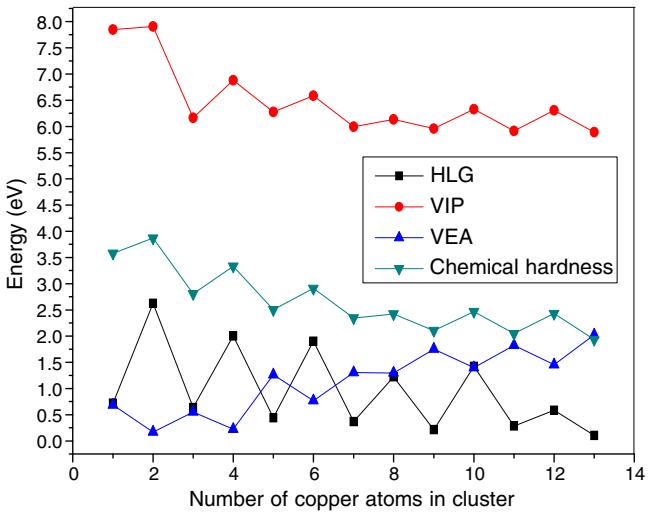

Figure 5. Size dependence of HLG, VIP, VEA and chemical hardness for Cu_nH_2 cluster.

find that the VIP and HLG of even-numbered Cu_nH_2 cluster are larger than those of adjacent odd-numbered Cu_nH_2 cluster, and the VEA of even-n Cu_nH_2 cluster is smaller than that of adjacent odd-n Cu_nH_2 cluster. The VIPs, HLGs and VEAs of Cu_nH_2 clusters show an obvious odd–even oscillation (see figure 5), indicating that the even-numbered Cu_nH_2 cluster is relatively more stable than the neighbouring odd-numbered Cu_nH_2 cluster electronically and chemically.

In addition to above parameters, the maximum hardness principle (MHP) also can be used to characterize the relative stability of a system.[37,38] In density functional theory, the chemical hardness (η) of an electronic system is defined as the second derivative of energy (E) with respect to the number of electrons (N) at constant external potential, $V(\vec{r})$.[39]

$$\eta = \frac{1}{2}\left(\frac{\partial^2 E}{\partial N^2}\right)_{V(\vec{r})} = \frac{1}{2}\left(\frac{\partial \mu}{\partial N}\right)_{V(\vec{r})},$$

where μ is the chemical potential of the system.

Using the finite difference approximation, chemical hardness η can be approximated as[39]

$$\eta = \frac{\mathrm{VIP} - \mathrm{VEA}}{2},$$

where VIP and VEA are the vertical ionization potential and vertical electron affinity of the chemical system.[39]

Based on this finite difference approximation, the chemical hardness for the lowest energy structures of Cu_nH_2 clusters are calculated, the results are listed in table 2 and shown in figure 5. It is easy to be found that as the cluster size increases, a common odd–even oscillation of chemical hardness also can be observed clearly. This picture is consistent with the odd–even oscillations of VIPs, HLGs and VEAs. According to the maximum hardness principle (MHP),[37,38] it also proves again that the even-numbered Cu_nH_2 cluster with higher chemical hardness is relatively more stable than the neighbouring odd-numbered Cu_nH_2 cluster. This pronounced odd–even oscillation pattern of HLG, VIP, VEA and chemical hardness also can be observed for pure gold clusters,[40–44] pure silver clusters[45] and pure copper clusters.[12] It also can be exhibited from the adsorption behaviour of H binding onto small copper clusters[13] and small gold clusters,[4] CO binding onto small gold clusters[46] and NCO species binding onto small silver clusters.[47] This alternation is due to the spin-pairing effect well-known for Au, Ag, Cu, and alkali metal clusters. As coinage metal atoms possess filled d-shells, they display electronic structure behaviour largely determined by the half-filled bands of nearly free s electrons. Thus, it is not surprising that all that coinage metal clusters exhibit size dependencies in physical properties that are similar to those observed in alkali metal clusters, and that they are more akin to alkali metal clusters than open d-shell transition element clusters.[48] This oscillation is, however, so much more pronounced in gold clusters than in alkali clusters that all even-sized gold clusters would almost be classified as magic clusters as they exhibit second difference cluster energies larger than zero.[41]

The interaction between small copper cluster and hydrogen molecule also can be reflected through charge transfer. By performing the Mulliken population analysis (MPA)[49] and natural orbital population analysis (NPA),[50,51] the effective charges on two H atoms of Cu_nH_2 clusters are listed in table 3 comparatively. Some previous calculations have proven that the natural orbital population analysis may provide a more accurate description for the charge distributions in a cluster than the Mulliken population analysis.[52–55] Obviously, the values obtained from NPA are larger than those obtained from MPA, indicating that much more charge transfers might take place between two H atoms

Table 3. Charge transfer between two H atoms and Cu_n for the lowest energy Cu_nH_2 clusters by performing Mulliken population analysis (MPA) and natural orbital population analysis (NPA).

Cluster	MPA		NPA		Cluster	MPA		NPA	
	H	H	H	H		H	H	H	H
CuH_2	0.006	0.006	0.011	0.011	Cu_8H_2	0.057	0.055	0.112	0.107
Cu_2H_2	0.083	0.083	0.101	0.101	Cu_9H_2	0.053	0.053	0.120	0.120
Cu_3H_2	0.057	0.058	0.091	0.095	$Cu_{10}H_2$	−0.064	−0.064	−0.122	−0.122
Cu_4H_2	0.054	0.052	0.109	0.102	$Cu_{11}H_2$	−0.086	−0.088	−0.134	−0.147
Cu_5H_2	0.055	0.059	0.160	0.172	$Cu_{12}H_2$	−0.085	−0.085	−0.147	−0.134
Cu_6H_2	0.071	0.074	0.114	0.124	$Cu_{13}H_2$	−0.050	−0.065	−0.109	−0.129
Cu_7H_2	0.059	0.059	0.103	0.103					

and Cu_n. Not only for Mulliken population analysis, but also for natural orbital population analysis, the values of charge transfer suggest a mechanism to favour electron donation for Cu_nH_2 (n = 1–9) clusters and electron back-donation for Cu_nH_2 (n = 10–13) clusters, that is, for Cu_nH_2 (n = 1–9) clusters, charge transfers from H_2 molecule to copper cluster and for Cu_nH_2 (n = 10–13) clusters, charge transfers from copper cluster to H_2 molecule, corresponding to molecular adsorption in Cu_nH_2 (n = 1–9) clusters and dissociative adsorption in Cu_nH_2 (n = 10–13) clusters, respectively. It seems that the mechanism of electron back-donation is more favourable to the dissociative adsorption. Remarkably, the greater charge transfer often leads to larger adsorption energy. This can be confirmed by Cu_nH_2 clusters. The greatest charge transfer takes place in $Cu_{11}H_2$ cluster with the largest adsorption energy and the smallest charge transfer takes place in CuH_2 cluster with the smallest adsorption energy. This indicates that greater charge transfer gives more electron pairing chance for Cu_n cluster and is also more favourable to the hydrogen molecule adsorption onto Cu_n cluster.

For a cluster, the number of electrons in the HOMO determines its ground-state electronic configuration. By orbital occupation analysis, we can find that the HOMOs of even-numbered Cu_nH_2 clusters with even number of valence electrons are fully occupied by the majority spin and minority spin electrons, which lead to the ground states of these clusters with closed electronic shell (see table 4) and are stable remarkably. But, the HOMOs of odd-numbered Cu_nH_2 clusters with odd number of electrons are occupied partially only by majority spin electrons and have open electronic shells (see table 4). According to the Jahn–Teller theorem, these clusters have the tendency to distort further toward lower symmetry so as to remove their degeneracy and lower their energy.[56] However, we must point out that the distorted cluster may also increase its degeneracy and have high spin multiplicity if it possesses a decreased total energy. It depends on a compromise between the decreasing of total energy and increasing of degeneracy, this compromise will decide whether or to what extent the Jahn–Teller distortion may take place.[57]

In order to understand the nature of chemical bonding in these systems, we have plotted the spatial orientations of HOMO for Cu_nH_2 clusters in figure 6. At first glance, the HOMOs of these clusters are delocalized obviously with a contribution from all atoms in the cluster. It is believed that this obvious delocalization phenomenon is the reflection of scalar relativistic effect. The strong s–d orbital hybridization between Cu atoms or between Cu atom and H atom is very obvious. When these s–d level exchanges occur, the Kubas-type interaction between copper atoms and H_2 characterized by forward donation of the bonding electron in H_2 to the partially filled transitional metal d orbital and back donation from the transitional metal atom to the σ^* anti-bonding orbital of H_2 becomes dominant and may provide a stronger and more stable configuration.[35,58–63] Such sigma-bonded Cu_n–H_2 complexes have binding energies intermediate between physisorption and chemisorption energies, which is desirable for fast kinetics.[61] For this reason, it may be ideal in hydrogen storage systems designed for room temperature applications.[36] Meanwhile, we can also find that

Table 4. Calculated highest vibrational frequencies of Cu–Cu, Cu–H and H–H mode for the lowest geometries of Cu_nH_2 clusters, pure Cu_n clusters and single H_2 molecule.

Cluster	ν_{Cu-Cu}(cm^{-1})	ν_{Cu-H}(cm^{-1})	ν_{H-H}(cm^{-1})	Cluster	ν_{Cu-Cu}(cm^{-1})	ν_{Cu-H}(cm^{-1})	ν_{H-H}(cm^{-1})
H_2			4387.2	Cu_8H_2	659.1	884.0	3631.5
CuH_2	768.4	316.0	4005.4	Cu_8	270.9	937.6	3406.4
Cu_2H_2	273.2	903.3	3533.2	Cu_9H_2	706.4	1040.0	1526.8
Cu_2	674.8	931.9	3025.8	Cu_9	258.9	1108.7	1383.3
Cu_3H_2	257.7	957.5	2976.4	$Cu_{10}H_2$	435.0	1070.6	1483.5
Cu_3	559.1	879.3	3364.1	Cu_{10}	251.0	1022.2	1565.5
Cu_4H_2	269.5	793.3	3850.4	$Cu_{11}H_2$	473.3		
Cu_4	625.8	735.9	3892.7	Cu_{11}	295.5		
Cu_5H_2	278.1			$Cu_{12}H_2$	384.0		
Cu_5	684.4			Cu_{12}	275.1		
Cu_6H_2	280.9			$Cu_{13}H_2$	598.7		
Cu_6	702.1			Cu_{13}	279.9		
Cu_7H_2	251.3						
Cu_7							

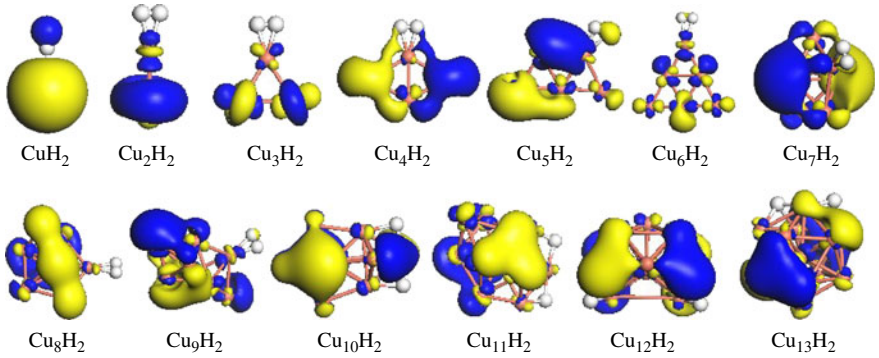

Figure 6. The spatial orientation of HOMO for Cu_nH_2 (n = 1–13) clusters.

the cluster-hydrogen seldom appears in the HOMO of almost all Cu_nH_2 clusters due to the low orbital energy of hydrogen. Hydrogen molecule adsorption onto small copper cluster often can be seen as partly involving an excitation to a formerly unoccupied orbital in the cluster, since the open shell has to be 'pushed up' when the cluster-hydrogen bond is formed. The same argument also can be found in connection with the bond preparation method used in the cluster surface model.[64]

3.3 *Frequency analysis*

Many experiments on the adsorption behaviour of small transitional metal clusters are based on the FTIR method and focused on the vibrational frequency of different mode in the adsorption system. In table 4 and figure 7, we give the highest frequencies of Cu–Cu, Cu–H, H–H mode for Cu_nH_2 clusters and Cu–Cu mode for pure Cu_n clusters, H–H mode for single H_2 molecule, respectively. It is easy to be found that the highest vibrational frequency of Cu–Cu mode for Cu_nH_2 cluster is significantly higher than that of Cu–Cu mode for corresponding pure Cu_n cluster, the highest vibrational frequency of H–H mode for Cu_nH_2 cluster is obviously lower than that of H–H mode for single H_2 molecule. This indicates that the Cu–Cu interaction is strengthened and the H–H interaction is weakened obviously after adsorption. It is also consistent with the shortening of Cu–Cu bond-length and the lengthening of H–H bond-length. Meanwhile, we can also find that the size dependence of the highest vibrational frequencies of Cu–H mode is approximately parallel to the size dependences of Cu–H bond-lengths and adsorption energies. $Cu_{11}H_2$ cluster has the maximum value of 1108.7 cm^{-1} and CuH_2 cluster has the minimum value of 316.0 cm^{-1}, corresponding to the shortest Cu–H bond-length, the largest adsorption energy in $Cu_{11}H_2$ cluster and the longest Cu–H bond-length, the smallest adsorption energy in CuH_2 cluster, respectively. It confirms that the strongest adsorption might belong to $Cu_{11}H_2$ cluster and the weakest adsorption might belong to CuH_2 cluster. Furthermore, the highest vibrational frequency of H–H mode has the opposite variation tendency of Cu–H mode (see figure 7). That is to say, the higher the highest vibrational frequency of Cu–H mode is, the lower the highest vibrational frequency of H–H mode will be, which leads to the stronger Cu–H interaction and the higher reactivity of H_2.

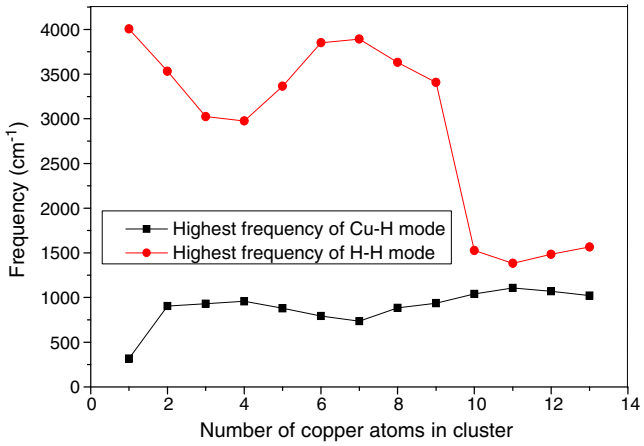

Figure 7. Size dependence of the highest frequency of Cu–H mode and H–H mode for Cu_nH_2 cluster.

3.4 *Magnetic properties*

Finally, we discuss here the magnetic properties of Cu_nH_2 clusters. From table 5, we can see that all the pure Cu_n clusters and Cu_nH_2 clusters prefer low spin multiplicity (M = 1 for even-numbered Cu_n clusters and even-numbered Cu_nH_2 clusters, M = 2 for odd-numbered Cu_n clusters and odd-numbered Cu_nH_2 clusters). The even-numbered pure Cu_n clusters and

Table 5. Electronic configuration, spin multiplicity, magnetic moment and $<S^2>$ values of the lowest energy Cu_nH_2 clusters.

Cluster	Electronic configuration	Magnetic moment(μ_B)			M		$<S^2>$	
		Cu_n	H_2	total	Cu_n	Cu_nH_2	Cu_n	Cu_nH_2
CuH_2	open	0.964	0.036	1.000	2	2	0.751	0.764
Cu_2H_2	closed	0.000	0.000	0.000	1	1	0.000	0.000
Cu_3H_2	open	0.942	0.058	1.000	2	2	0.754	0.770
Cu_4H_2	closed	0.000	0.000	0.000	1	1	0.000	0.000
Cu_5H_2	open	0.968	0.032	1.000	2	2	0.752	0.769
Cu_6H_2	closed	0.000	0.000	0.000	1	1	0.000	0.000
Cu_7H_2	open	1.000	0.000	1.000	2	2	0.759	0.772
Cu_8H_2	closed	0.000	0.000	0.000	1	1	0.000	0.000
Cu_9H_2	open	0.989	0.011	1.000	2	2	0.760	0.774
$Cu_{10}H_2$	closed	0.000	0.000	0.000	1	1	0.000	0.000
$Cu_{11}H_2$	open	0.965	0.035	1.000	2	2	0.757	0.769
$Cu_{12}H_2$	closed	0.000	0.000	0.000	1	1	0.000	0.000
$Cu_{13}H_2$	open	0.989	0.011	1.000	2	2	0.761	0.778

even-numbered Cu_nH_2 clusters are found to exhibit zero magnetic moment and the odd-numbered pure Cu_n clusters and odd-numbered Cu_nH_2 clusters are found to possess magnetic moment with the value of 1 μ_B (mainly contributed by Cu_n). The odd–even alterations of magnetic moments for pure Cu_n clusters and Cu_nH_2 clusters are very obvious and similar with previous work[65], in which the pronounced even–odd alteration of magnetic moments for Au_7H_n clusters can be observed. This odd-even alteration of magnetic moments may be served as the material with tunable code capacity of '0' and '1'[65] can be simply understood by considering the electron pairing effect between the valence electron of $Cu3d^{10}4s^1$ and the valence electron of $H1s^1$. Previous studies[66–68] have shown that charge transfer and the hybridization of valence electrons stemming from host and impurity influence the local magnetic moment significantly. The local magnetic moment of the scandium doped gold system is quenched because of the strong pairing effect between the scandium 3*d* electrons and gold 6*s* electrons. It is similar with the situation of the pairing effect between the 3*d*4*s* electrons of Cu_n and the 1*s* electron of H_2 in Cu_nH_2 clusters of our work.

Spin-contamination is a well-known problem for open-shell systems which can drastically reduce the accuracy of *ab initio* computations that are based on the Unrestricted Hartree–Fock (UHF) wavefunction formalism.[69,70] An unrestricted wavefunction allows the separate alpha and beta spin orbitals to relax such that they are not equal in energy. This ultimately means that the unrestricted determinant is not an eigenfunction of the S_2 operator, as higher multiplicity spin states are allowed to mix into the wavefunction. Some error may be introduced into the calculations.[71–73] In order to investigate the influence of spin-contamination, the $<S^2>$ values of the lowest energy pure Cu_n clusters and Cu_nH_2 clusters are given in table 5. Expectedly, the $<S^2>$ values for all singlet spin states are zero, indicating that no spin-contamination can be found in the closed-shell systems of even-numbered Cu_n clusters and even-numbered Cu_nH_2 clusters. The $<S^2>$ values of doublet spin states for the open-shell systems of odd-numbered Cu_n clusters and odd-numbered Cu_nH_2 clusters are close to the exact value of 0.750 for doublet and the deviations are less than 10%. It is inferred that the influences of spin-contamination in these open-shell systems are in a small scale and can be acceptable. In fact, for many doublet systems a value of 0.750–0.800 is expected and causes a negligible loss in accuracy for the calculations.[73–77] Recently, Yamaguchi *et al*. have proposed an approximate spin-projection (AP) method in order to eliminate the spin contamination error from the total energy of the broken symmetry low spin state.[78,79]

4. Conclusions

In this paper, an all-electron scalar relativistic calculation on Cu_nH_2 ($n = 1$–13) clusters has been performed by using density functional theory with the generalized gradient approximation at PW91 level. The main conclusions are as follows:

(i) After the adsorption of H_2 molecule, the Cu–Cu interaction is strengthened and the H–H interaction is weakened, the enhancement of reactivity

of H_2 is obvious, appearing as the shortening of Cu–Cu bond-length and the lengthening of H–H bond-length. The strongest adsorption exists in $Cu_{11}H_2$ cluster and the weakest adsorption exists in CuH_2 cluster. Compared with pure Cu_n clusters, only the Cu_{11} structure in $Cu_{11}H_2$ cluster is distorted obviously.

(ii) The hydrogen molecule adsorption is more favourable to enhancement of Cu–Cu interaction than the hydrogen atom adsorption. The dissociative adsorption only takes place in some Cu_nH_2 ($n = 10$–13) clusters of our work and not in all Cu_nH_2 ($n = 2$–15) clusters like ref.[11] These discrepancies may be understood in terms of the electron pairing effect and the scalar relativistic effect.

(iii) The odd–even alteration of magnetic moments is observed in Cu_nH_2 ($n = 1$–13) clusters and may be served as the material with tunable code capacity of '0' and '1' by adsorbing hydrogen molecule onto odd or even-numbered small copper clusters.

Acknowledgement

This work was supported by the Nature Science Foundation of Chongqing city. No. CSTCĄ|2007BB4137.

References

1. Melius C F, Upton T H and Goddard W A 1978 *Solid. State. Commun*. **28** 501
2. Upton T H and Goddard W A 1979 *Phys. Rev. Lett*. **42** 472
3. Bauschlicher C W, Bagus P S and Schaefer H F 1978 *IBM. J. Research. Dev*. **22** 213
4. Phala S, Klatt G and Steen E V 2004 *Chem. Phys. Lett*. **395** 33
5. Okumura M, Kitagawa Y, Haruta M and Yamaguchi K 2005 *Appl. Catal: A Gen* **291** 37
6. Wu X, Senapati L, Nayak S K, Selloni A and Hajaligol M 2002 *J. Chem. Phys* **117** 4010
7. Kadossov E, Justin J, Lu M, Rosenmann D, Ocola L E, Cabrini S and Burghaus U 2009 *Chem. Phys. Lett*. **483** 250
8. Ding X, Yang J L, Hou J G and Zhu Q S 2005 *J. Mol. Struct*. (THEOCHEM) **755** 9
9. De Oliveira L A, Wolf A and Schuth F 2001 *Catal. Lett*. **73** 157
10. Ricart J M, Torras J, Rubio J and Illas F 1997 *Surf. Sci*. **374** 31
11. Guvelioglu G H, Ma P P, He X Y, Forrey R C and Cheng H S 2005 *Phys. Rev. Lett*. **94** 026103
12. Guvelioglu G H, Ma P P, He X Y, Forrey R C and Cheng H S 2006 *Phys. Rev.* **B73** 155436
13. Triguero L, Wahlgren U, Boussard P and Siegbahn P 1995 *Chem. Phys. Lett*. **237** 550
14. Campos L P 2007 *J. Mol. Struct*. (THEOCHEM) **815** 63
15. Campos L P 2008 *J. Mol. Struct*. (THEOCHEM) **851** 15
16. Holmgren L, Andersson M and Rosen A 1998 *Chem. Phys. Lett*. **296** 167
17. Wang F and Li L M 2004 *Acta. Phys. Chim. Sin*. **20** 966
18. Autschbach J, Siekierski S, Seth M, Schwerdtfeger P and Schwarz W H E 2002 *J. Comput. Chem*. **23** 804
19. Jain P K 2005 *Struct. Chem*. **16** 421
20. Fernandez E M, Soler J M, Garzon L L and Balbas C 2004 *Phys. Rev. B* **70** 165403
21. Kuang X J, Wang X Q and Liu G B 2010 *Indian. J. Phys*. **84** 245
22. Orita H, Itoh N and Inada Y 2004 *Chem. Phys. Lett*. **384** 271
23. Lee Y S and McLean A D 1982 *J. Chem. Phys*. **76** 735
24. Datta S N and Ewig C S 1982 *Chem. Phys. Lett*. **85** 443
25. Jackson K A 1993 *Phys. Rev. B* **47** 9715
26. Lammers U and Borstel G 1994 *Phys. Rev.* **B49** 17360
27. Erkoc S and Shaltaf R 1999 *Phys. Rev*. **A60** 3053
28. Massobrio C, Pasquarello A and Car R 1995 *Chem. Phys. Lett*. **238** 215
29. Kabir M, Mookerjee A and Bhattacharya A K 2004 *Phys. Rev*. **A69** 043203
30. Matulis V E, Ivashkevich O A and Gurin V S 2004 *J. Mol. Struct*. (Theochem) **681** 169
31. Spasov V A and Lee T H 1993 *J. Chem. Phys*. **99** 6308
32. Spasov V A, Lee T H and Ervin K M 2000 *J. Chem. Phys*. **112** 1713
33. Kouteck V B, Gaus J, Guest M F, Cespiva L and Kouteck J 1993 *Chem. Phys. Lett*. **206** 528
34. Corma A, Boronat M, González S and Illas F 2007 *Chem. Commun*. (Cambridge) **125** 3371
35. Kubas G J 2001 *J. Organometal. Chem.* **635** 37
36. Hoang K A and Antonelli D M 2009 *Adv. Mater*. **21** 1787
37. Parr R G and Chattaraj P K 1991 *J. Am. Chem. Soc*. **113** 1854
38. Pearson R G 1987 *J. Chem. Edu* **64** 561
39. Parr R G and Pearson R G 1983 *J. Am. Chem. Soc*. **105** 7512
40. Hakkinen H and Landman U 2000 *Phys. Rev. B* **62** R2287
41. Assadollahzadeha B and Schwerdtfegera P 2009 *J. Chem. Phys*. **131** 06430
42. Zhao J, Yang J L and Hou J G 2003 *Phys. Rev. B* **67** 085404
43. Majumder C and Kulshreshtha S K 2006 *Phys. Rev. B* **73** 155427
44. Nijamudheen A and Ayan Datta 2010 *J. Mol. Struct*. (Theochem) **945** 93
45. Hualei Zhang A and Dongxu Tian 2008 *Comput. Mater. Sci* **42** 462
46. Phala N S, Klatt G and Steen E V 2004 *Chem. Phys. Lett*. **395** 33
47. Zhao S, Ren Y L, Wang J J and Yin W P 2009 *J. Mol. Struct*. (Theochem) **897** 100

48. Heer W A D 1993 *Rev. Mod. Phys*. **65** 611
49. Mulliken R S 1955 *J. Chem. Phys*. **23** 1841
50. Reed A E and Weinhold F 1983 *J. Chem. Phys*. **78** 4066
51. Reed A E, Weinstock R B and Weinhold F 1985 *J. Chem. Phys*. **83** 735
52. Han J G and Hagelberg F 2001 *Chem. Phys*. **263** 255
53. Han J G and Hagelberg F 2001 *J. Mol. Struct*. (THEOCHEM.) **549** 165
54. Han J G and Hagelberg F 2002 *Struct. Chem*. **13** 173
55. Han J G, Sheng L S, Zhang Y W and Morales J A 2003 *Chem. Phys*. **294** 211
56. Eberhart M E, Handley R C and Johnson K H 1984 *Phys. Rev*. **B29** 1097
57. Yang J L, Toigo F and Wang K L 1994 *Phys. Rev. B* **50** 7915
58. Kim G B, Jhi S H, Lim S and Park N J 2009 *Phys. Rev. B* **79** 155437
59. Kubas G J 2007 *Chem. Rev*. **107** 4152
60. Kubas G J 2007 *Proc. Natl. Acad. Sci. USA* **104** 6901
61. Kubas G J 2006 *Science* **314** 1096
62. Weck P F, Dhilip Kumar T J, Kim E and Balakrishnan N 2007 *J. Chem. Phys* **126** 094703
63. Szarek P, Urakami K, Zhou C G, Cheng H S and Tachibana A 2009 *J. Chem. Phys*. **130** 084111
64. Panas L, Siegbahn P and Walhgren U 1987 *Chem. Phys*. **112** 325
65. Zhang M, He L M, Zhao L X, Feng X J, Cao W and Luo Y H 2009 *J. Mol. Struct*. (THEOCHEM) **911** 65
66. Torres M B, Fernández E M and Balbás L C 2006 *Phys. Rev*. **B71** 155412
67. Majumder C, Kandalam A K and Jena P 2006 *Phys. Rev*. **B74** 205437
68. Janssens E, Tanaka H, Neukermans S, Silverans R E and Lievens P 2004 *Phys. Rev*. **B69** 085402
69. Yamaguchi K 1990 in: R. Carbo, M. Klobukowski (eds.), *Self-consistent field theory and applications*, Amsterdam: Elsevier, p. 727
70. Szabo A 1996 Ostlund, modern quantum chemistry, New York: Dover Publications, Inc., N.S., pp. 205–230 (Chapter 3)
71. Hajgató B, Szieberth D, Geerlings P, De Proft F and Deleuze M S 2009 *J. Chem. Phys*. **131** 224321
72. Yamaguchi K, Kawakami T, Takano Y, Kitagawa Y, Yamashita Y and Fujita H 2002 *Int. J. Quantam Chem*. **90** 370
73. Williams T G, DeYonker N J, Ho B S and Wilson A K 2011 *Chem. Phys. Lett*. **504** 88
74. Okumura M, Kitagawa Y, Yabushita H, Saito T and Kawakami T 2009 *Catal. Today*. **143** 282
75. Bendikov M, Duong H M, Starkey K, Houk K N, Carter E A and Wudl F 2004 *J. Am. Chem. Soc*. **126** 7416
76. Ipatov A, Cordova F, Doriol L J and Casida M E 2009 *J. Mol. Struct*. (Theochem) **914** 60
77. Shalabi A S, AbdelHalim W S and Ghonaim M S 2011 *Physica B* **406** 397
78. Yamaguchi K, Takahara Y, Fueno T and Houk K N 1988 *Theor. Chim. Acta*. **73** 337
79. Yamanaka S, Okumura M, Nakano M and Yamaguchi K 1994 *J. Mol. Struct*. (THEOCHEM) **310** 205